

Numerical Field Analysis for Determining Universal Motor's Performance Curves

MILOŠ BEKOVIĆ, ANTON HAMLER

Faculty of Electrical Engineering and Computer Science

Laboratory for Applied Electromagnetic

University of Maribor

Smetanova ul. 17, 2000 Maribor,

SLOVENIJA

Abstract: - In this paper a three-dimensional (3D) numerical magnetic field analysis of universal motor (UM) is treated. For this purpose the software package OPERA Vector Fields was used. The field computation for four different loads and for each load a three different rotor positions was made. A mathematical procedure for calculation the electromechanical characteristics which basis on post processing of the results of numerical magnetic field calculation is described. Comparison between measured and calculated performance curves is presented.

Key-Words: - numerical analysis, finite element method, universal motor, performance curves,

1 Introduction

Small UM are in fact single-phase series motors that can run successfully on AC or DC power supply. Due to the low manufacture costs, good performance characteristics and easy maintenance they are the most obvious solution for variety of domestic appliances. They drive washing machines, air-conditioning compressors, fans, pumps, vacuum cleaners hand tools, and so on. Literally millions of single-phase machines are manufactured each year. Manufacturers tend to lower the costs of production without jeopardizing the electromechanical performance of motor. From electrical point of view the good performance stands for high efficiency witch is conditional whit low losses. That kind of demands suggests implementation of optimizing process of certain parts of motor during a construction phase. At each step of optimizing process electromechanical characteristics have to be calculated as criteria of good performance.

With suggested method performance curves can be determent before the motor is actually built therefore we need accurate magnetic field analysis. This paper presents 3D analysis of UM model in software package OPERA for selected loads and rotor positions.

In post processor some field parameters where obtained so that vector diagram of UM shown in Fig. 1 could be calculated.

2 Governing Equations of UM

For the basic explanation of UM a vector diagram for certain rotor speed n as shown in Fig. 1. can be taken. On real axis lies the current vector I , while the supply voltage vector U is rotated by angle φ and it is the geometric sum of voltages U_f and U_a . For the stator (field) winding (FW) the voltage balance can be expressed with equation:

$$U_f = R_f I + jX_{\sigma f} I + E_{tr}, \tag{1}$$

and the armature voltage in armature winding (AW)

$$U_a = R_a I + jX_a I + \Delta U_c + E_r + E_a. \tag{2}$$

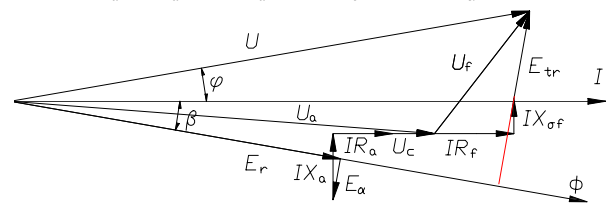


Fig. 1. Vector diagram of a UM

R_f and R_a are windings resistances, $X_{\sigma f}$ is the leakage reactance of the FW and X_a reactance of the AW. ΔU_c is the voltage drop on the motor's brushes while E_r is the rotational induced voltage produced by pulsating field, which can be calculated

$$E_r = \frac{1}{\sqrt{2}} \frac{p n z}{a 60} \Phi_m. \tag{3}$$

In (3) the p represents number of poles, z is the number of active bars in AW, a is the number of parallel branches and Φ_m is main flux. In FW there is also a transformer induced voltage, where its effective value is

$$E_{tr} = \sqrt{2} \pi f w_v \Phi_m \quad (4),$$

and w_v is FW number of turns. Motor's brushes are shifted from neutral zone by angle α to reduce influence of armature reaction so, that influence of transformer induced voltage of coils in area 2α must be included.

$$E_\alpha = \sqrt{2} \pi f \frac{4\alpha}{360} \frac{z}{4a} \Phi_m \quad (5),$$

If the voltage vectors from Fig. 1 are projected on real axis and multiplied with current I , power distribution of UM as seen in Fig. 2 appears.

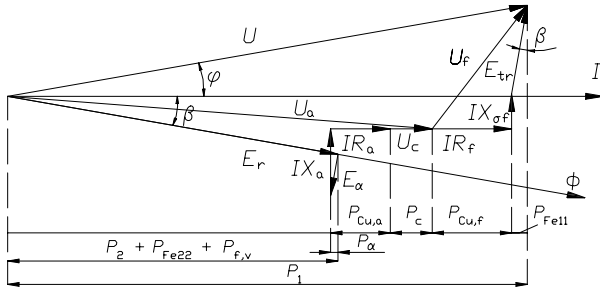


Fig. 2. Power distribution and losses of UM

The average torque value of the of UM when the main flux lags behind the current by angle β can be calculated

$$M_{avg\sim} = \frac{pz}{2\sqrt{2}a\pi} \Phi_m I \cos \beta. \quad (6),$$

Value (6) does not represent mechanical torque, because the losses of the friction and ventilation $P_{f,v}$ plus rotor steel losses P_{Fe22} divided with the mechanical angular speed of rotor Ω must be subtracted.

$$M_{loss} = \frac{P_{Fe22} + P_{f,v}}{\Omega}. \quad (7),$$

Mechanical torque on the motor shaft is

$$M = M_{avg\sim} - M_{loss} \quad (8),$$

and the output power

$$P_2 = M \Omega. \quad (9),$$

More of the UM's theory can be found in [1],[2],[3] and [4].

3 Analyzed Motor

Motor analyzed in this paper was universal motor with parameters exposed in table 1.

Table 1. Data of the analysed UM

rated input power	450W
rated voltage, frequency	230V / 50Hz
rated current	2.071A
moment of inertia	$0.1322 \cdot 10^{-3} \text{ kgm}^2$

The FW on the two silent stator poles have 250 turns on each pole with resistance of 5.1Ω per pole at 20°C . Rotor has 24 coils and each coil has 46 turns and total armature resistance at nominal temperature is 10.69Ω .

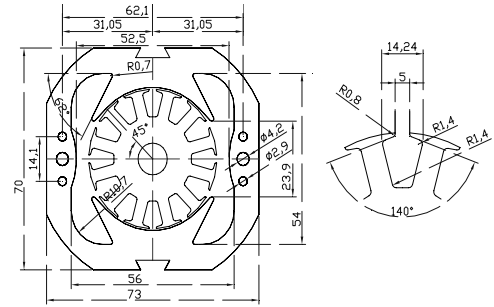


Fig. 3. Cross section of analyzed UM

Since analyzed UM is intending to run on AC power supply its stator and rotor iron core must be laminated to reduce eddy current effect. Dimension of stator and rotor laminated steel sheets with all geometry data used in UM can be seen on Fig. 3.

Fig. 4 shows the scheme of AW and arrows which indicate current direction at given brush position.

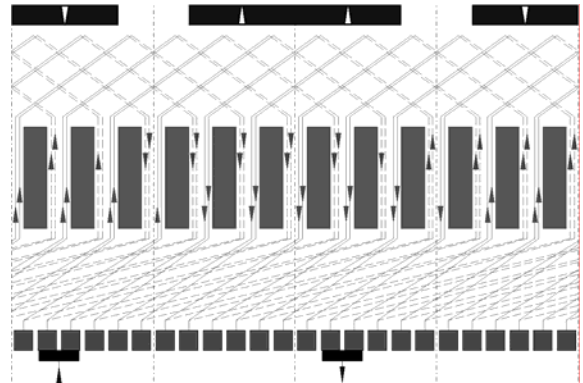


Fig. 4. Scheme of AW with 12 slots

4 Magnetic Field Analysis of UM

Numerical field calculation of the magnetic field was carried out by finite element software package OPERA. Model contained approximately 646 000 elements and 659 000 nodes.

4.1 Pre processing

In this phase of preparation for calculation the geometrical model of problem (UM) is built, cell properties are defined and some other parameters are determined. Building a geometrical model include designing basic elements of the motor; laminated stator and rotor magnetic core, motor shaft, FW and AW.

Fig. 5. shows geometrical model used for numerical analysis. On stator's salient poles there are 2 FW and in 12 rotor slots there are 24 AW according to Fig. 4.



Fig. 5. Geometrical model of UM

Next step before calculation is defining properties of areas.

For the magnetic parts of the stator and rotor core, shaft and two screws total potential type ($\Psi, J=0$) must be selected, for areas with air (air gap, rotor slots and surrounding air) reduced potential ($\Phi, J \neq 0$) is selected. For the magnetic package of the UM the steel manufacturers BH curve and the direction of the lamination was defined.

Since the FEM basis on a model composed of finite elements, surface and volume mesh must be created before the computation as seen on Fig. 6. Maximal size of finite element for certain areas and level of polynomial approximating functions is prescribed. This indirectly influence to the accuracy of the filed analysis. In areas, where higher field changes are predicted thicker mesh is demand (air gap). The whole problem of filed computation of UM was enveloped with surrounding air where because of visualization only half of it is visible and to which boundary conditions where prescribed.

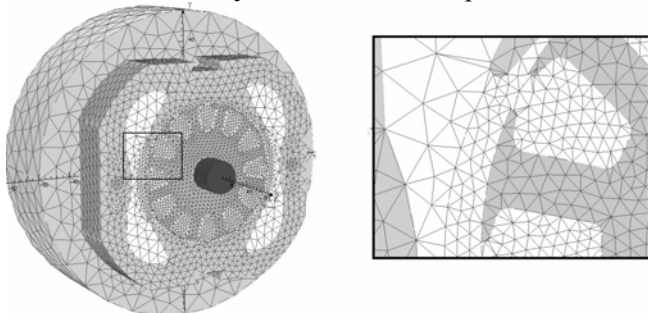


Fig. 6. Discrete model of UM with only half of surrounding air and no windings

For computation motor's characteristic a several different load points are necessary hence this analysis was performed for four equidistance load currents. Solving field problems with numerical methods the current distribution in coils must be known. Because of the series connection of FW and AW load current is half of field current so that current density used in field and armature coils was prescribed as

$$J_f = \frac{\sqrt{2} I N_f}{S_f}, \quad J_a = \frac{\sqrt{2} I N_a}{2S_a} \quad (10)$$

where S indicate surface of model coils and N is actual number of turns of FW and AW.

In commutating coils with assumed linear commutation average value of current in these coils short circuit by the brushes equals zero.

On Fig. 4 can be seen, that brush is wider than the width of single commutator segment and at given rotor position short circuits one coil per brush, together two. When shifting rotor for 7.5° brush covers three segments short circuits two coils per brush, together four and at additional shift for 7.5° commutator again covers only two coils. For each of four load current three discreet rotor positions ($0^\circ, 7.5^\circ$ and 15°) analysis where performed so that in later analysis average value of variable (Φ_m, L, W, \dots) for each load from all three rotor positions was calculated.

4.2 Post processing

Solution of FEM returns the potential value in discreet points of the problem. Post processing of the results was carried out in software module OPERA Post processor. With selecting type of analysis (TOSCA MAGNETOSTATIC) program determent local field parameters (B, H). Purpose of this numerical field analysis was to determent some integral system parameters such as magnetic flux Φ , forces and torque (F, M), energy and co energy of the system (W, W') and inductance (L).

For each load current value of the main flux Φ_m that enters into the rotor via air gap was calculated. Program enables computation of surface integrals of selected variables or mathematical expressions and with known relationship that

$$\Phi = \iint_S B \, dS \quad (11)$$

Φ_m can be calculated. S is the surface surrounding half of the air gap from first brush to second along the whole axial length of iron core.

In (1) appears stator's leakage inductance voltage drop $IX_{\sigma f}$ where $X_{\sigma f} = L_{\sigma f} \omega$ is leakage inductive reactance. Inductivity $L_{\sigma f}$ was calculated with (12) where value of the leakage flux is Φ_σ was calculated with (11) and the surface S represened surrounding surface of the stator coil.

$$L_{\sigma f} = \frac{\Phi_\sigma N_f}{I} \quad (12)$$

Armature's inductivity L_a can be determent with expression for the rotor field energy, where it is

$$W_m = \frac{\Psi I}{2} \rightarrow \Psi = \frac{2 W_m}{I} \quad (13)$$

and for inductivity states the equation

$$L_a = \frac{\Psi}{I} = \frac{2W_m}{I^2} = \frac{2}{I^2} \int_{V_a} \left(\int_B HdB \right) dV. \quad (14)$$

On Fig. 2. can be seen, that angle β between I and Φ_m can be calculated from iron losses P_{Fe11}

$$P_{Fe11} = E_v I \sin \beta. \quad (15)$$

Stator's and rotor's iron losses where calculated with (16) and (17), where in those equation appears product B^2V . Those two values where calculated in program since enables computation of volume integrals of certain variables or mathematical expressions.

$$P_{Fe11} = 0.95 p_{Fe} \rho_{Fe} \left(\frac{f_1}{50} \right)^2 \iiint_{V_s} B_{mod}^2 dV_s \quad (16)$$

$$P_{Fe22} = 0.95 p_{Fe} \rho_{Fe} \left(\frac{f_2}{50} \right)^2 \iiint_{V_r} B_{mod}^2 dV_r \quad (17)$$

Where p_{Fe} stands for core losses (W/kg @ 50 Hz), ρ_{Fe} is steel density (kg/dm³) and these two parameters where provided by steel manufacturer. 0.95 stands for packaging factor of laminated steel and value f_2 represents rotor's frequency, which was calculated as

$$f_2 = \frac{p n}{60}. \quad (18)$$

Opera Post processor enables various presentations of field variables or expressions. For example it enables figure plot of variable along line. On Fig. 7 there's air gap magnetic flux density for example of only FW supplied and FW and AW supplied. The influence of armature reaction on the resulting magnetic field axis which is shifted against the direction of the rotation can be observed.

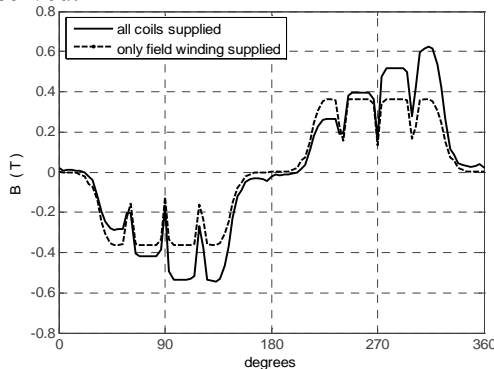


Fig. 7. Calculated magnetic flux density in air gap around rotor showing armature reaction

5. Computation of Performance Curves

For calculating performance curves of UM vector diagram of voltage distribution from Fig. 1 had to be known. Sequence of parameters computation can be seen on Fig. 8 flow chart. In first part motor's voltage distribution was calculated.

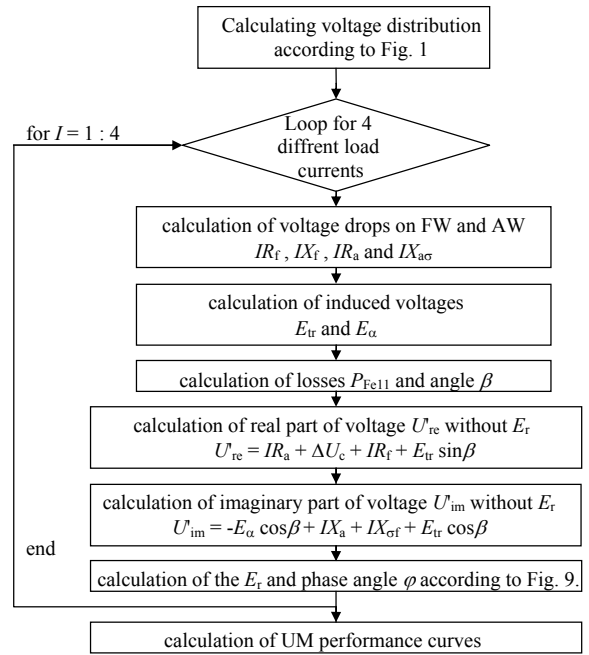


Fig. 8. Flow chart of the computation

The only unknown variable in vector diagram from Fig. 1 stays E_r or more exactly motors revolutions n at certain load. If we now plot real and imaginary vectors of known voltages U_{re} , U_{im} angle β and U and position of unknown E_r and angle ϕ in Fig. 9.

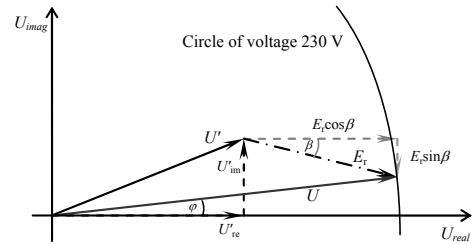


Fig. 9. Vector diagram of known and unknown voltages

If equation for voltage triangle from Fig. 9 is set E_r and phase angle ϕ can be calculated form (20).

$$U^2 = (U_{re}' + E_r \cos \beta)^2 + (U_{im}' - E_r \sin \beta)^2 \quad (20)$$

By knowing voltage E_r the whole voltage vector diagram from Fig. 1 is known. With (3) motor's revolution was calculated. With (6), (7) and (8) torque on motor's shaft, input power (21) and output power (9) was calculated.

$$P_1 = U I \cos \phi \quad (21)$$

Efficiency of the motor η is determent as the ratio between output power and input power.

$$\eta = \frac{P_2}{P_1} \quad (22)$$

Result of numerical field analysis and mathematical computation are the variables, with who performance curves of the UM can be plotted. Since the whole computation was performed on real motor model, we had

the chance to measure its characteristics so, that we could compare described method with measured results. Fig. 10. shows the current speed characteristics $I=f(n)$ for calculated and measured values.

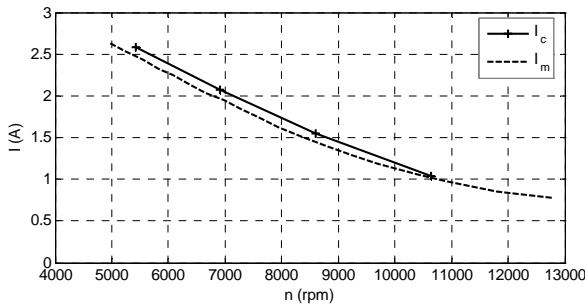


Fig. 10. Current-speed curves; computed curves are compared with measured curves

Fig. 11. shows the mechanical torque-speed characteristics $M=f(n)$ while Fig. 12. shows input and output power-speed curves.

On Fig. 13. there's comparison between measured and calculated efficiency $\eta=f(n)$.

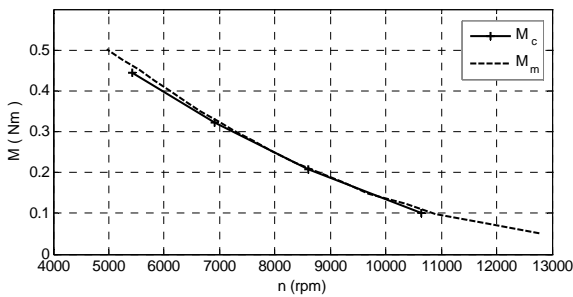


Fig. 11. Torque-speed curves; computed curves are compared with measured curves

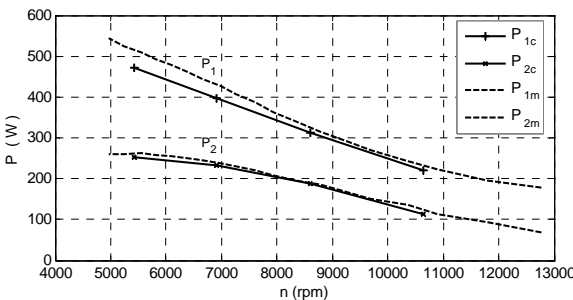


Fig. 12. Input power-speed and output power-speed curves; computed curves are compared with measured curves

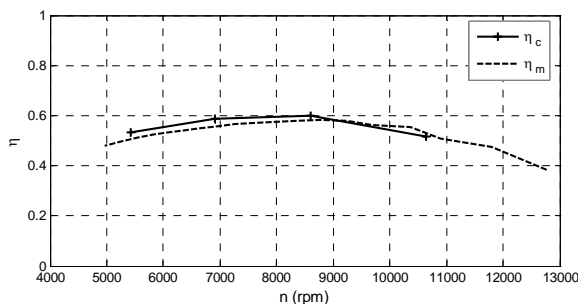


Fig. 13. Torque-speed curves; computed curves are compared with measured curves

In Fig. from 10 to 13 subscript c in legend denotes calculated and m denotes measured variable.

When calculating the load characteristics are for losses $P_{f,v}$ taken experimentally determined values and not numerically. More of this method can be found in [7].

6. Conclusions

This paper presents one possible approach for determining performance curves of UM. Here is suggested procedure how from field variables and geometry data determine some parameters needed to calculate performance curves that agrees very well with measured curves. Only weakness of this method is long computation times for field analysis since it is 3D example.

References

- [1] B. Jurković, Z. Smolčić, Kolektroski strojevi, školska knjiga Zagreb, 1986, Udžbenici sveučilišta u Zagrebu
- [2] D. Dinić, Kolektroske Mašine, III. Deo, specialne kolektroske mašine, Begred 1970
- [3] G. McPherson, R.D. Laramore: An Introduction to Electrical Machines and Transformers, second edition
- [4] M. Kostenko, L. Pitorovsky: Electrical Machines in two volumes, vol.II, Alternating Current Machines, Mir Publishers, MOSCOW 1969
- [5] G.Henneberger, G.Asche, D.Rödder: "Computer Modelling of an Universal Motor by numerical Field Analysis and Dynamic simulation"
- [6] Roderick N. Ebben: "Performance Curves of a Series DC Motor Predicted Using Parametric Finite Element Analysis", IEEE TRANSACTIONS ON MAGNETICS. vol. 35, no. 3, May 1999
- [7] F. Avčin, P. Jereb, Preizkušanje električnih strojev, Založba življenje in tehnika, Ljubljana 1966